Symbolic-Numeric Stability Investigations of Jameson's Schemes for the Thin-layer Navier-Stokes Equations

V.G. Ganzha(*), E.V. Vorozhtsov,
Institute of Theoretical and Applied Mechanics,
Russian Academy of Sciences, Novosibirsk 630090, Russia
(*) At the moment GH–Universität, Kassel

J. Boers and J.A. van Hulzen
Department of Computer Science, University of Twente,
P.O.Box 217, 7500AE Enschede, The Netherlands

Abstract

The Navier-Stokes equations governing the three-dimensional flows of a viscous, compressible, heat-conducting gas and augmented by turbulence modeling present the most realistic model for gas flows around the elements of aircraft configurations. We study the stability of one of the Jameson's schemes of 1981, which approximates the set of five Navier-Stokes equations completed by the turbulence model of Baldwin and Lomax. The analysis procedure implements the check-up of the necessary von Neumann stability criterion. It is shown with the aid of the proposed symbolic-numeric strategy that the physical viscosity terms in the Navier-Stokes equations have a dominant effect on the sizes of the stability region in comparison with the heat conduction terms. It turns out that the consideration of turbulence with the aid of eddy viscosity model of Baldwin and Lomax has an insignificant effect on the size of the necessary stability region.

1 Introduction

The rapid advances in computer hardware and architecture achieved during the last decade enabled computational fluid dynamicists to solve many complicated two- and three dimensional flow problems with the aid of the numerical integration of the Navier-Stokes equations. The Navier-Stokes equations represent a more complicated model of fluid flows than the Euler equations, because they take into account also the effects of viscosity and heat conduction along with the compressibility effect.

The complex structure of the Navier-Stokes equations makes increased demands on the computational efficiency of the numerical discretization techniques for these equations. In the case of the solution of stationary fluid dynamics problems the increase of the computational efficiency is achieved mainly by the increase of a maximum time step allowed by the stability of the numerical pseudo-unsteady method. Therefore, much effort was spent in the development of implicit difference methods for the Navier-Stokes equations. The linear von Neumann stability analysis shows that these methods are unconditionally stable, that is they allow unrestricted time steps. But in practice limitations for the time step arise, which are dictated by the accuracy of the numerical solution [1]. In addition, the implementation of implicit schemes may become difficult in the cases of complicated geometries of the spatial domains, in which the viscous gas flow is to be modeled.

The idea of using the explicit time-stepping Runge-Kutta schemes for the numerical integration of the Euler and Navier-Stokes equations, which was proposed by A. Jameson [2], offers a good possibility to extend the time steps when allowed by the stability. For example, the five-stage Jameson's scheme for the Euler equations allows a Courant number of 4, which is by a factor of 4 larger than for the well-known MacCormack scheme [3]. V.N. Vatsa [4] gives further advantages of the Jameson's schemes: (i) decoupling of spatial and temporal differencing renders the steady-state solutions independent of the Courant number; (ii) these schemes are highly vectorizable on vector processors such as the Cray XMP and VPS-32, thereby making them very efficient from a computational point of view.

Our choice of one of the Jameson's scheme for the stability investigation is caused by the above mentioned advantages of these schemes as well as by the following two attractive features of these schemes.

(a) The amplification matrix G of these schemes, which is obtained as an important part of the Fourier stability analysis, is represented by a polynomial in some other matrix. This simplifies the further stability investigation.

(b) In the particular case of the absence of the physical viscosity and heat conduction the Navier-Stokes equations revert to the familiar Euler equations. In this particular case it is possible to obtain even the closed-form analytic necessary stability conditions for the Jameson's schemes [5]. This is important for the verification of a symbolic-numerical method, which we describe below.

Despite the relatively simple structure of the amplification matrix corresponding to Jameson's schemes there are still no results on the stability of these schemes as applied to the Navier-Stokes equations. In [5, 6] we have analyzed the stability of two three-stage Jameson's schemes applied

ISAAC 94 - 7/94 Oxford England UK

to the model two-dimensional advection-diffusion equation

$$\frac{\partial u}{\partial t} + A\frac{\partial u}{\partial x} + B\frac{\partial u}{\partial y} = \nu\left(\frac{\partial^2 u}{\partial x^2} + \frac{\partial^2 u}{\partial y^2}\right), \qquad (1.1)$$

where A and B are the constant components of the advection velocity vector along the x- and y-axes, respectively; ν is the diffusion coefficient, $\nu = const > 0$. The numerical data on the stability region boundaries were fitted in [5, 6] by certain analytic formulas, which are very convenient for their use in practical computations by the three-stage Jamesson's schemes.

We have proposed in [7] a new symbolic-numerical method for the stability investigation of difference schemes approximating the Euler equations with two or three spatial variables. This method reduces the von Neumann stability analysis to the algebra of resultants. The coordinates of points of the stability region boundary are then computed with the aid of the numerical solution of certain optimization problems.

Now we present an extension of the approach given in [7] to the stability investigation of the four-stage Jameson's scheme applied to the thin-layer variant of the Navier-Stokes equations in three spatial variables.

2 Governing Equations

The curvilinear surfaces of airplane wings, the flow around which was considered in [4], require using curvilinear coordinates η and ζ instead of the rectangular Cartesian coordinates x, y and z. Therefore the thin-layer unsteady Navier-Stokes equations in [4] are given in general curvilinear coordinates ξ, η and ζ. These equations have a much more complicated form than the Navier-Stokes equations in rectangular Cartesian coordinates x, y and z, due to the presence of metric terms like the derivatives $\partial x/\partial\xi$, $\partial x/\partial\eta$, ..., $\partial z/\partial\xi$, $\partial z/\partial\eta$, $\partial z/\partial\zeta$ and the Jacobian of the transformation from x, y, z to ξ, η, ζ.

In connection with the foregoing we consider in here the thin-layer Navier-Stokes equations in the rectangular Cartesian coordinates x, y and z. Let us assume that we want to solve numerically how a viscous gas flows over a flat plate. Let us place the Ox and Oz axes on the plate surface such that the Oz axis is parallel with the mainstream vector. Then the Oy axis is parallel with a normal to the plate surface. Therefore it will intersect the boundary layer, which develops in a viscous fluid flow over the plate. Since the dominant viscous effects at high Reynolds number turbulent flow arise from viscous diffusion normal to the body surface, a thin-layer assumption can be employed, where only the viscous diffusion terms normal to the body surface are retained [4]. The governing equations for a coordinate system fixed in time can then be written in the conservation law-form, and as presented in [4]:

$$\frac{\partial \vec{u}}{\partial t} + \frac{\partial \vec{F}(\vec{u})}{\partial x} + \frac{\partial \vec{G}(\vec{u})}{\partial y} + \frac{\partial \vec{H}(\vec{u})}{\partial z} = \frac{\partial \vec{S}(\vec{u})}{\partial y}, \qquad (2.1)$$

where

$$\vec{u} = \begin{bmatrix} \rho \\ \rho u \\ \rho v \\ \rho w \\ \rho E \end{bmatrix}, \vec{F}(\vec{u}) = \begin{bmatrix} \rho u \\ p + \rho u^2 \\ \rho uv \\ \rho uw \\ \rho uH \end{bmatrix}, \qquad (2.2)$$

$$\vec{G}(\vec{u}) = \begin{bmatrix} \rho v \\ \rho uv \\ p + \rho v^2 \\ \rho vw \\ \rho vH \end{bmatrix}, \vec{H}(\vec{u}) = \begin{bmatrix} \rho w \\ \rho uw \\ \rho vw \\ p + \rho w^2 \\ \rho wH \end{bmatrix}, \qquad (2.3)$$

$$\vec{S}(\vec{u}) = \sqrt{\gamma}\frac{M_\infty}{Re_\infty}\begin{bmatrix} 0 \\ \mu\bar{\varepsilon}u_y \\ \frac{4}{3}\mu\bar{\varepsilon}v_y \\ \mu\bar{\varepsilon}w_y \\ \frac{\mu\bar{\varepsilon}}{2}(u^2+v^2+w^2)_y + \\ \frac{\mu\bar{\varepsilon}}{3}vv_y + \frac{\gamma}{\gamma-1}\frac{\mu\tilde{\varepsilon}}{\sigma}T_y \end{bmatrix}. \qquad (2.4)$$

Here ρ is the fluid density, u, v and w are the fluid velocity components along the axes x-,y- and z-axis, respectively; p is the pressure; $E = \varepsilon + (u^2+v^2+w^2)/2$, ε is the specific internal energy. In the preceding set of equations, distances have been nondimensionalized by a reference length L; density, pressure, and viscosity by their respective freestream values; and velocities by a reference velocity $u_{ref} = a_\infty/\sqrt{\gamma}$, where a_∞ is the freestream speed of sound; and enthalpy H by u^2_{ref}. γ is the ratio of the gas specific heats, $\gamma = 1.4$ for the air. For an ideal gas, the enthalpy is then given by the relation

$$\rho H = (\frac{\gamma}{\gamma-1})p + \rho(\frac{u^2+v^2+w^2}{2}).$$

M_∞ is the freestream Mach number; Re_∞ is the freestream Reynolds number.

In the governing equations presented here, the effect of turbulence is accounted for through the concepts of an eddy viscosity and eddy conductivity. In the momentum equations, the molecular viscosity μ is replaced by the effective viscosity μ_e,

$$\mu_e = \mu + \mu_t = \mu(1 + \frac{\mu_t}{\mu}) = \mu\bar{\varepsilon}, \qquad (2.5)$$

where $\bar{\varepsilon} = 1 + \mu_t/\mu$ and μ_t denotes the turbulent viscosity. Similarly, in the energy equation, the molecular conductivity k is replaced by the effective conductivity k_e,

$$k_e = k + k_t = \frac{C_p}{\sigma}\mu + \frac{C_p}{\sigma_t}\mu_t = \frac{C_p\mu}{\sigma}(1 + \frac{\sigma}{\sigma_t}\frac{\mu_t}{\mu}) = \frac{C_p\mu}{\sigma}\tilde{\varepsilon} = k\tilde{\varepsilon},$$

where

$$\tilde{\varepsilon} = 1 + \frac{\sigma}{\sigma_t}\frac{\mu_t}{\mu} \qquad (2.6)$$

Here σ is the laminar Prandtl number and σ_t the turbulent Prandtl number.

3 The Four-Stage Scheme of Jameson

In accordance with the general construction of the Jameson's schemes [2] let us introduce the operator P of differencing in the spatial variables x, y and z:

$$P\vec{u} = \frac{\vec{F}^n_{i+1,j,k} - \vec{F}^n_{i-1,j,k}}{2h_1} + \frac{\vec{G}^n_{i,j+1,k} - \vec{G}^n_{i,j-1,k}}{2h_2} + \frac{\vec{H}^n_{i,j,k+1} - \vec{H}^n_{i,j,k-1}}{2h_3} - \frac{\vec{S}^n_{i,j+1,k} - \vec{S}^n_{i,j-1,k}}{2h_2} \qquad (3.1)$$

Here h_1, h_2 and h_3 are the steps of uniform rectangular grid along the axes x, y and z, respectively; $\vec{F}^n_{i,j,k} = \vec{F}(\vec{u}^n_{i,j,k})$, etc.; $\vec{u}^n_{i,j,k} = \vec{u}(ih_1, jh_2, kh_3, n\tau)$, τ is the time step. In [4] the artificial dissipation terms have been added to the operator $P\vec{u}$ (3.1) to avoid the appearance of oscillations in the vicinity of shock waves and stagnation points. In our present consideration we will not introduce these extra terms in $P\vec{u}$, although the consideration of these terms is not impossible within the framework of our symbolic-numeric approach.

In accordance with the idea of the lines method for the solution of PDEs we now consider instead of the PDE system (2.1) the ODE system

$$\frac{d\vec{u}}{dt} + P\vec{u} = 0. \tag{3.2}$$

To advance the solution from time level n to $n+1$ using four stages, the scheme takes the following form:

$$\begin{aligned} \vec{u}^{(0)} &= \vec{u}^n \\ \vec{u}^{(1)} &= \vec{u}^{(0)} - \frac{\tau}{4}P\vec{u}^{(0)} \\ \vec{u}^{(2)} &= \vec{u}^{(0)} - \frac{\tau}{3}P\vec{u}^{(1)} \\ \vec{u}^{(3)} &= \vec{u}^{(0)} - \frac{\tau}{2}P\vec{u}^{(2)} \\ \vec{u}^{n+1} &= \vec{u}^{(0)} - \tau P\vec{u}^{(3)}. \end{aligned} \tag{3.3}$$

The scheme of Eq. (3.3) is a modified form of the classical Runge-Kutta scheme and is very attractive for three-dimensional problems, since it requires only two time levels of the solution vector in memory. It is pointed out in [4] that (3.3) is fourth-order accurate in time for linear problems and is second-order accurate in time for nonlinear problems.

Since the Fourier method for stability analysis is applicable only to linear difference schemes, we have to linearize the operator $P\vec{u}$ (3.1) before proceeding to the stability investigation of the Jameson's scheme (3.3), (3.1). Let us denote by $\bar{P}$ the linearized version of the operator P. Then we may write that

$$\begin{aligned} \bar{P}\vec{u} = {} & A_1(\vec{u})\frac{\vec{u}^n_{i+1,j,k} - \vec{u}^n_{i-1,j,k}}{2h_1} + \\ & A_2(\vec{u})\frac{\vec{u}^n_{i,j+1,k} - \vec{u}^n_{i,j-1,k}}{2h_2} + \\ & A_3(\vec{u})\frac{\vec{u}^n_{i,j,k+1} - \vec{u}^n_{i,j,k-1}}{2h_3} - \\ & A_4(\vec{u})\frac{\vec{u}^n_{i,j+1,k} - 2\vec{u}^n_{i,j,k} + \vec{u}^n_{i,j-1,k}}{h_2^2} \end{aligned} \tag{3.4}$$

The expressions for the Jacobian matrices $A_1(\vec{u}) = \partial\vec{F}(\vec{u})/\partial\vec{u}$, $A_2(\vec{u}) = \partial\vec{G}(\vec{u})/\partial\vec{u}$ and $A_3(\vec{u}) = \partial\vec{H}(\vec{u})/\partial\vec{u}$ may be found in [7]. The temperature T, which enters the vector of viscous terms (2.4), does not enter explicitly the components of the solution vector $\vec{u}$ in (2.2). Therefore, before proceeding to the derivation of the matrix A_4 in (3.4), we at first express the derivatives of T with respect to y in terms of the derivatives of functions p and ρ. Let us denote by $\bar{p}, \bar{\rho}$ and $\bar{T}$ the nondimensionalized functions for pressure, density and temperature, respectively. In accordance with the above described procedure of non-dimensionalization we may write that

$$\begin{aligned} \bar{p} &= \frac{p}{p_\infty} = \frac{p}{(\gamma-1)\rho_\infty\varepsilon_\infty} = \frac{p}{(\gamma-1)\rho_\infty c_v T_\infty} \\ &= \frac{R\rho T}{(c_p - c_v)\rho_\infty T_\infty} = \bar{\rho}\bar{T}, \end{aligned} \tag{3.5}$$

where the universal gas constant $R = c_p - c_v$ and c_p and c_v are the gas specific heats. From (3.5) we know that $T = p/\rho$ (the bars over p, ρ and T are omitted), therefore,

$$\frac{\partial T}{\partial y} = \frac{1}{\rho}\frac{\partial p}{\partial y} - \frac{p}{\rho^2}\frac{\partial \rho}{\partial y}. \tag{3.6}$$

We now substitute the right hand side of the expression (3.6) instead of $\partial T/\partial y$ into the vector $\vec{S}(\vec{u})$ in (2.4) and compute the entries of the Jacobi matrix $A_4(\vec{u}) = \partial\vec{S}(\vec{u})/\partial\vec{u}$. As a result we obtain that

$$A_4(\vec{u}) = \sqrt{\gamma}\frac{M_\infty}{Re_\infty}\frac{\mu\tilde{\varepsilon}}{\rho}. \tag{3.7}$$

$$\begin{pmatrix} 0 & 0 & 0 & 0 & 0 \\ -u & 1 & 0 & 0 & 0 \\ -\frac{4v}{3} & 0 & \frac{4}{3} & 0 & 0 \\ -u & 0 & 0 & 1 & 0 \\ s_{51} & u(1-\alpha) & v(\frac{4}{3}-\alpha) & w(1-\alpha) & \frac{\gamma\tilde{\varepsilon}}{\sigma\rho\bar{\varepsilon}} \end{pmatrix},$$

where

$$s_{51} = -(u^2 + \frac{4}{3}v^2 + w^2) - \frac{a^2\tilde{\varepsilon}}{(\gamma-1)\sigma\bar{\varepsilon}} + \frac{\alpha}{2}(u^2+v^2+w^2),$$

$$\alpha = \frac{\gamma\tilde{\varepsilon}}{(\gamma-1)\sigma\bar{\varepsilon}}, a = \sqrt{\gamma p/\rho},$$

that is a is the local sound speed. It is assumed in the subsequent stability analysis of the difference scheme (3.3), (3.4) that the elements of the matricies $A_j(\vec{u}), j = 1\ldots4$, are constant.

Let us now consider important concerning of the choice of certain nondimensional quantities $\kappa_1, \kappa_2, \ldots, \kappa_M$ $(M \geq 1)$, in the domain of the variation of which the necessary stability region will be determined. It was found in [7] that in the inviscid case (that is when $\mu = 0$ in (3.7)) the stability region may be determined in the space of the following nondimensional quantities:

$$\begin{aligned} \kappa_1 = \frac{a\tau}{h_1}, \kappa_2 = \frac{u\tau}{h_1}, \kappa_3 = \frac{v\tau}{h_1}, \kappa_4 = \frac{w\tau}{h_1}, \\ \kappa_5 = \frac{h_1}{h_2}, \kappa_6 = \frac{h_1}{h_3}, \kappa_7 = \gamma \end{aligned} \tag{3.8}$$

where $a = \sqrt{\gamma p/\rho}$ is adiabatic sound speed. Let us now determine the form of those nondimensional quantities which are due to the presence of viscous terms in (3.4). For this purpose let us look at the equation for determining $\vec{u}^{(1)}$ in (3.3). The components of the vector $\vec{u}^{(0)}$ are nondimensional (see above). Therefore, the components of the vector $\tau P\vec{u}^n$ should also be nondimensional. Let us now look at the vector $\tau\partial/\partial y[\vec{S}(\vec{u})]$, where $\vec{S}(\vec{u})$ is determined by (2.4). It is easy to see that only two additional nondimensional quantities, κ_8 and κ_9, arise:

$$\kappa_8 = \sqrt{\gamma}\frac{M_\infty}{Re_\infty}\frac{\tau\mu\bar{\varepsilon}}{h_1^2\rho}, \quad \kappa_9 = \frac{\tilde{\varepsilon}}{\bar{\varepsilon}\sigma}. \tag{3.9}$$

Note that the case $\kappa_9 = 0$ corresponds to the absence of heat conduction in the fluid. It is also to be noted that the physical nondimensional quantities, the numbers M_∞ and Re_∞, enter the formulas (3.9) only in the form of the fraction M_∞/Re_∞.

Let us now obtain the amplification matrix G of the difference scheme (3.3), (3.4). Since the coefficients of the operator $\bar{P}\vec{u}$ (3.4) are constant, the difference scheme (3.3),

(3.4) can be written down after the elimination of the intermediate values $\vec{u}^{(1)}, \vec{u}^{(2)}$ and $\vec{u}^{(3)}$ as a two-level scheme

$$\vec{u}^{n+1} = C\vec{u}^n, \tag{3.10}$$

where C is the step operator,

$$C = I - \tau\bar{P} + \frac{(\tau\bar{P})^2}{2!} - \frac{(\tau\bar{P})^3}{3!} + \frac{(\tau\bar{P})^4}{4!}. \tag{3.11}$$

In accordance with the Fourier method let us now substitute a solution of the form

$$\vec{u}(x,y,z,t) = \vec{u}_0 \exp\{i(k_1x + k_2y + k_3z - \omega t)\}$$

into scheme (3.10), where k_1, k_2, k_3 are the real wavenumbers, ω is wave frequency, $\vec{u}_0$ is a constant vector and $i = \sqrt{-1}$. Let

$$Z = \mathcal{F}(-\tau\bar{P}) \tag{3.12}$$

for the Fourier symbol of the operator $-\tau\bar{P}$. Then we easily obtain the amplification matrix G of the scheme (3.10) as

$$G = I + Z + \frac{1}{2!}Z^2 + \frac{1}{3!}Z^3 + \frac{1}{4!}Z^4. \tag{3.13}$$

The form of the matrix Z is also easily obtained by taking into acount the formula (3.4):

$$\begin{aligned} Z &= \mathcal{F}(-\tau\bar{P}) \qquad (3.14)\\ &= -i\tau\sum_{j=1}^{3}\frac{(\sin\xi_j)A_j}{h_j} - \frac{2\tau}{(h_2^2)}(1-\cos\xi_2)A_4, \end{aligned}$$

where $\xi_j = k_jh_j, j = 1,2,3$. Let us denote by $\lambda_j, j = 1\ldots5$, the eigenvalues of the matrix Z, and let $\mu_j, j = 1\ldots5$, be the eigenvalues of the amplification matrix G. Then in accordance with (3.13) we have that

$$\mu_j = 1 + \lambda_j + \frac{1}{2}\lambda_j^2 + \frac{1}{6}\lambda_j^3 + \frac{1}{24}\lambda_j^4. \tag{3.15}$$

As is known, the necessary von Neumann stability condition has the form

$$|\mu_j| \le 1 + O(\tau),\ j = 1\ldots5. \tag{3.16}$$

In what follows we will search for such a necessary stability region, in which the inequalities

$$|\mu_j| \le 1,\ j = 1\ldots5, \tag{3.17}$$

are satisfied. The inequalities (3.17) obviously imply the von Neumann inequalities (3.16).

It is easy to find from the condition (3.17) the necessary von Neumann stability condition of scheme (3.3), (3.4) in the inviscid case by using the fact that the linear combination $\beta_1A_1 + \beta_2A_2 + \beta_3A_3$ of gas dynamical matrices can be diagonalized by one matrix entering the similarity transformation [8]. The inviscid necessary stability condition may be written down in the form [5]

$$\begin{aligned} &|u|\tau/h_1 + |v|\tau/h_2 + |w|\tau/h_3 + \\ &\frac{a\tau}{h_1}\sqrt{1 + (h_1/h_2)^2 + (h_1/h_3)^2} \le 2\sqrt{2}. \end{aligned} \tag{3.18}$$

In terms of the nondimensional quantities (3.8) this formula can be rewritten as

$$|\kappa_2| + |\kappa_3|\kappa_5 + |\kappa_4|\kappa_6 + \kappa_1\sqrt{(1 + \kappa_5^2 + \kappa_6^2)} \le 2\sqrt{2}. \tag{3.19}$$

The constant $C = 2\sqrt{2}$ in the right hand side of the necessary stability condition (3.19) is called the Courant number. Note that $C = 1$ in the case of the well-known MacCormack's scheme of 1969 [3], see [7]. It was noted [4] that in the case of three-dimensional viscous flow problems the Courant number limit is somewhat lower than $2\sqrt{2}$ due to the presence of large cell aspect ratios κ_5 and κ_6 and viscous dissipation.

4 A Symbolic-Numeric Strategy to determine the Necessary Stability Region

We want to be able to determine a necessary stability region (NSR) for which (3.17) is satisfied. So, we have to compute eigenvalues of the amplification matrix G of scheme (3.10), given by (3.13) as a polynomial in the matrix Z, which in turn is defined by (3.14). Instead of G itself we can and will use the matrix Z and its eigenvalues and test whether (3.17) is satisfied. Since determination of a NSR requires many eigenvalues computations the efficiency of production and use of eigenvalue computation code is important.

To begin with we look closer at the (5,5)-matrix Z. Its entries are multivariate rational functions in elements of the set

$$V = \{sa, sb, cb, sc, \kappa_1, \kappa_2, \ldots, \kappa_9, \tau, h_1\}$$

Here $sa = \sin\xi_1$, $sb = \sin\xi_2$, $cb = \cos\xi_2$ and $sc = \sin\xi_3$. Like done in [7] we can associate with Z a matrix EZ of exponents $\epsilon_{i,j}$, if the entries of Z are given by $z_{i,j} = f_{i,j}.q^{\epsilon_{i,j}}$ where $q = \frac{\tau}{h}$ and $\frac{\partial f_{i,j}}{\partial q} = 0$ for $i = 1\ldots5$ and $j = 1\ldots5$. Visual inspection of Z showed:

$$EZ = \begin{pmatrix} 0 & 1 & 1 & 1 & 2\\ -1 & 0 & 0 & 0 & 1\\ -1 & 0 & 0 & 0 & 1\\ -1 & 0 & 0 & 0 & 1\\ -2 & -1 & -1 & -1 & 0 \end{pmatrix}$$

Taking into account the structure of EZ it is easy to show that the matrix $Z_1 = TZT^{-1}$, where $T = diag(1,q,q,q,q^2)$, does not depend on q. The matrix Z_1 has the same set of eigenvalues as the matrix Z and can be obtained formally from Z by setting $q = 1$ in Z. The entries of Z are thus reduced to expressions in the κ_i, $i = 1\ldots9$ and the sprectral variables ξ_i with period $T_i = 2\pi$, $i = 1\ldots3$.

We determine the eigenvalues of Z numerically. Like done in [7] we used REDUCE [9] to create Z. We can use GENTRAN [10] and SCOPE 1.5 [11][1] to produce optimized Fortran 77 code for computing values for the entries of Z for permissible inputs. Once being able to compute the entries of Z we can also compute its eigenvalues, using an IMSL[2] or a NAG[3] library routine.

The entries of Z are multivariate expressions. We have some freedom in deciding how to organize Z-entry computations, and thus eigenvalue computations. Six of the nine κ_i's can be replaced by numerical constants, the others can be viewed as free parameters. Let us denote these free parameters by κ_j, κ_k and κ_m. So for a specific 6-tuple of κ_i-substitutions the set V is further reduced to $V^* = \{sa, sb, cb, sc, \kappa_j, \kappa_k, \kappa_m\}$. We denote the resulting presentation of Z by Z^*. It are the entries of this Z^* we

[1] An earlier version of SCOPE was presented in [12].

[2] International Mathematical & Statistics Library, Inc. (IMSL).

[3] NAG Fortran Library Manual Mark 13, Numerical Algorithm Group, Oxford, 1988.

translate into numerical code. Let us assume that we want to determine the NSR in the parallelepiped

$$P : \{Min_i \leq \kappa_i \leq Max_i,\ i = j, k, m\}.$$

The Min_i and Max_i are given quantities. It can be seen from (3.14) that the entries of the amplification matrix (3.13) are periodic functions of ξ_1, ξ_2 and ξ_3 with equal periods $T_j = 2\pi, j = 1, 2, 3$. Therefore, let us further assume that we have a parallelepiped

$$\Pi : \{0 \leq \xi_j \leq T_j,\ j = 1, 2, 3\},$$

like P also in the three-dimensional Euclidian space E^3. We can construct a (κ_j, κ_k)-grid P_g in the (κ_j, κ_k)-plane, such that $Min_i \leq \kappa_i \leq Max_i$ for $i = j, k$. We can also construct a grid Π_g over Π. Each point in Π_g corresponds with a 4-tuple (sa, sb, cb, sc). We consider the numerical computation of eigenvalues of Z^* as the application of a function EV:

$$EV(Z^*, \kappa_j, \kappa_k, \kappa_m, \xi_1, \xi_2, \xi_3)$$

For a given pair of grid-values (p_x, π_y) with $p_x \in P_g$ and $\pi_y \in \Pi_g$ the entries of Z^* are reduced to univariate polynomials in κ_m. Permissible values of κ_m have to be selected from the interval $[Min_m, Max_m]$. If we apply EV for such a value of κ_m we obtain the set $\Lambda_{x,y}$ of eigenvalues of a specific presentation $Z_{x,y}$ of Z^*. Then (3.15) can be used to test wether $\Lambda_{x,y}$ produces a maximum $\mu_{x,y}$ of the absolute values of the eigenvalues of the corresponding amplification matrix $G_{x,y}$, which is bounded in accordance with (3.17). We now introduce a characteristic function:

$$\mathcal{C}(p_x, \kappa_m) = \begin{cases} 1 & \text{if } \forall_{\pi_y \in \Pi_g}\ \mu_{x,y} \leq 1. \\ -1 & \text{otherwise.} \end{cases}$$

The function $\mathcal{C}$ can be applied in a bisection process over $[Min_m, Max_m]$ for all $p_x \in P_g$ in the following way:

1. Let $min = Min_m$ and $max = Max_m$.
2. Compute $Signl = \mathcal{C}(p_x, min)$ and $Signr = \mathcal{C}(p_x, max)$
3. If $Signl = 1 \wedge Signr = 1$ then Deliver($\kappa_m = max$)
4. If $Signl = -1 \wedge Signr = -1$ then Deliver($\kappa_m = min$)
5. $ctr = (min + max)/2$
6. if $\mathcal{C}(p_x, ctr) = Signr$ then $max = ctr$ else $min = ctr$
7. if $abs(max - min) > eps$
   then goto 5 else Deliver($\kappa_m = ctr$)

We may assume for the presented applications that $\mathcal{C}(p_x, min) = -1 \wedge \mathcal{C}(p_x, max) = 1$ does not occur. All, thus produced $\kappa_m > Min_m$ define NSR-boundary points $(\kappa_j, \kappa_k, \kappa_m)$, associated with $p_x = (\kappa_j, \kappa_k)$. $\mathcal{C}(p_x, \kappa)$ requires many eigenvalue computations and leads to a triple $(\kappa_j, \kappa_k, \kappa_m)$, being one of the permissible P-points. All P-points are collected in a GNUPLOT [13] acceptable format in some file. This graphic tool is used to visualize the NSR.

In summary, the following symbolic-numeric strategy is adopted:

1. Use REDUCE 3.5 to generate $Z_{q=1}$.
2. Select a 6-tuple of κ_i-values and compute Z^*.
3. Use GENTRAN and SCOPE 1.5 for the generation of a Fortran 77 subroutine, defining how to compute the entries of Z^*.
4. Construct P_g and Π_g.
5. Iterate over all $p_x \in P_g$ to obtain the NSR-boundaries.
6. Use GNUPLOT 3.5 to visualize the NSR.

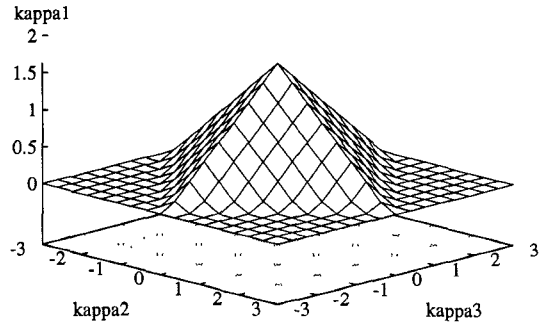

Figure 1: 3D section of the NSR for $\kappa_8 = \kappa_9 = 0$, $\kappa_7 = 1.4$, $\kappa_4 = 0$, $\kappa_5 = \kappa_6 = 1$.

5 Results and Discussion

We used the formula (3.19) as a test of the above presented symbolic-numeric strategy. In Fig. 1 we show the isometric picture of the necessary stability region computed for the case of an inviscid, non-heat-conducting gas.

The accuracy was set to $\varepsilon = 1/1000$ in the bisection process. It may be seen from Fig. 1 that the NSR boundary intersects the plane $\kappa_1 = 0$ along the line

$$|\kappa_2| + |\kappa_3|\kappa_5 = 2\sqrt{2}.$$

Thus the obtained numerical results agree with the analytical formula (3.19).

The most interesting case is that of a viscous, heat-conducting, compressible gas. The following questions are of interest here: (i) What is the influence of the gas viscosity and heat conduction on the sizes of the stability region? (ii) How do the cell aspect ratios κ_5 and κ_6 affect the necessary stability region? The cases $\kappa_5 \gg 1$ and $\kappa_6 \gg 1$ correspond to highly stretched cells of a spatial computing mesh. Thus by varying the values of κ_5 and κ_6 we can investigate the effects of the stretching of cells in some subregions of a general curvilinear grid, which was used in [4]. Our present investigation is restricted to the case of a rectangular uniform spatial computational grid. The cells of a general curvilinear grid possess also some skewness along with the stretching. To take into account the skewness effects we would have to consider in the coefficients of the difference equations all the metric terms involving the derivatives $\partial x/\partial\xi, \partial x/\partial\eta, \ldots, \partial z/\partial\xi, \partial z/\partial\zeta$ (see Section 2 above). This necessitates the development of a new stability analysis method, which is much more elaborate than the method for the case of a rectangular uniform grid.

For the inviscid case, it may be seen from (3.19) that the cell aspect ratios κ_5 and κ_6 affect significantly the stability

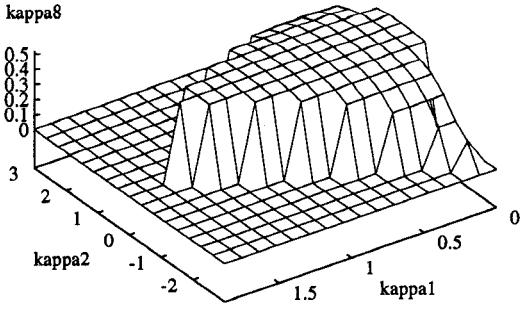

Figure 2: $\kappa_8 = \kappa_8(\kappa_1, \kappa_2)$, $\kappa_9 = 0$, $\kappa_5 = \kappa_6 = 1$, $\kappa_7 = 1.4$, $\kappa_3 = \kappa_4 = 0$.

region. For example, in the case $\kappa_5 = 2$, $\kappa_6 = 1$ the stability region proves to be compressed in the direction of the κ_3 axis and so one has the impression that the NSR is stretched along the κ_2 axis. In the case $\kappa_5 = 0.5$, $\kappa_6 = 1$ the NSR proves to be compressed in the direction of the κ_2 axis. In Fig.2 a 3D section of the NSR is presented for the case of a viscous, non-heat-conducting gas.

Note that the values of κ_1 cannot be negative due to the physical meaning of the sound speed in (3.8). It may be seen from Fig. 2 that the values of κ_8 on the NSR boundary are positive only over the region $\kappa_1\sqrt{1+\kappa_5^2+\kappa_6^2} + |\kappa_2| \le 2\sqrt{2}$ in the plane $\kappa_8 = 0$. This agrees with the formula (3.19).

We can also see from Fig. 2 that the NSR is symmetric with respect to the plane $\kappa_2 = 0$. The maximum stable value of κ_8 in Fig. 2 is the value $\kappa_8 = 0.53$, which is achieved at the point of the intersection of the $O\kappa_8$ axis with the NSR boundary. Let us find the exact value of κ_8 at $\kappa_1 = \kappa_2 = 0$ by using the formulas (3.8), (3.9), (3.13) and (3.14). At $\kappa_1 = \kappa_2 = \kappa_3 = \kappa_4 = 0$, $\kappa_9 = 0$ it is easy to see that only some entries of the matrix A_4 in (3.14) are different from zero, so that

$$Z = diag(0, \delta, \frac{4}{3}\delta, \delta, 0), \tag{5.1}$$

where

$$\delta = -2\kappa_5^2\kappa_8(1 - \cos\xi_2). \tag{5.2}$$

It follows from (5.1) that the eigenvalues $\lambda_j, j = 1, \ldots, 5$, of the matrix Z are expressed by the formulas

$$\lambda_{1,2} = 0, \lambda_{3,4} = \delta, \lambda_5 = \frac{4}{3}\delta. \tag{5.3}$$

We can see that all the eigenvalues λ_j are real and nonpositive by virtue of (5.2). Let us find the limitation from above for κ_8 from (3.17): $1 + \lambda_j + \frac{1}{2}\lambda_j^2 + \frac{1}{6}\lambda_j^3 + \frac{1}{24}\lambda_j^4 \le 1$. This inequality obviously leads to a simpler inequality

$$24 + 12\lambda_j + 4\lambda_j^2 + \lambda_j^3 \ge 0. \tag{5.4}$$

Consider the cubic equation

$$\lambda_j^3 + 4\lambda_j^2 + 12\lambda_j + 24 = 0.$$

In accordance with the Cardano's solution this equation has one real zero and two complex conjugate zeros. The real zero λ_{j0} is expressed by the formula

$$\begin{aligned}\lambda_{j0} &= \frac{1}{3}[\sqrt[3]{12\sqrt{269} - 172} - \sqrt[3]{12\sqrt{269} + 172} - 4] \\ &\approx -2.7852935.\end{aligned}$$

Therefore, we obtain with (5.2) and (5.3) the following limitation for κ_8 from the inequality (5.4):

$$\kappa_8 \le -3\lambda_{j0}/(8\kappa_5^2(1 - \cos\xi_2)). \tag{5.5}$$

As a function of ξ_2 the right hand side of (5.5) achieves its minimum at $\xi_2 = \pi$. At this value of ξ_2 we obtain from (5.5) the inequality

$$\kappa_8 \le -3\lambda_{j0}/(16\kappa_5^2). \tag{5.6}$$

Since $\kappa_5 = 1$ in the case of Fig. 2, we obtain from (5.6) that $\kappa_8 \approx 0.5222425$ at the point of the intersection of the $O\kappa_8$ axis with the NSR boundary. Thus the above analytical study confirms the results of Fig. 2, which have been obtained with the aid of the proposed symbolic-numerical method.

Let us now present a number of results for the case of a viscous, heat-conducting gas. In accordance with [14, 15] we may take the values $\sigma = 0.72$ for the laminar Prandtl number σ and $\sigma_t = 0.9$ for the turbulent Prandtl number σ_t in (2.6). The turbulent viscosity μ_t is small outside the turbulent boundary layers, therefore, $\bar{\varepsilon} \approx 1$, $\tilde{\varepsilon} \approx 1$ for the laminar flow regime. For this flow regime we can therefore take the value $\kappa_9 = 1/\sigma = 1/0.72$ in accordance with (3.9). Within the turbulent boundary layers we have that

$$\kappa_9 = \frac{\tilde{\varepsilon}}{\bar{\varepsilon}\sigma} = \frac{1}{\sigma}(1 + \frac{\sigma}{\sigma_t}\frac{\mu_t}{\mu})/(1 + \frac{\mu_t}{\mu}), \tag{5.7}$$

where $\mu_t > 0$ depends on the solution gradients [14, 15]. Since $\sigma/\sigma_t = 0.72/0.9 < 1$, we have from (5.7) that for the turbulent flow regime $0 < \kappa_9 < 1/\sigma \approx 1.388889$. The local solution gradients are different in different subdomains of the turbulent flow. We can take into account this effect, by considering different values of κ_9 in the range $0 < \kappa_9 < 1.388889$. We have performed such a parametric study for a number of values of κ_9. In Fig. 3 we present a 3D section of the NSR for the laminar flow case, that is when $\kappa_9 = 1/0.72$. Figs. 4,5 refer to the turbulent flow regime. The following conclusions may be drawn from the Figs. 3, 4 and 5:

- Fig. 3 shows that the height $\kappa_8(\kappa_1, \kappa_2)$ of the NSR boundary over the plane $\kappa_8 = 0$ remains nearly the same for different values of κ_9 and is equal to 0.53, as in the case $\kappa_9 = 0$ (see Fig. 2). This effect may be explained by the predominant role of the gas viscosity μ in the difference scheme (3.3), (3.4) when $\mu > 0, \kappa_9 > 0$.
- The points on the surface $\kappa_8(\kappa_1, \kappa_2)$ form a plateau of almost constant values, so that one can take approximately $\kappa_8 = 0.53$ on this plateau. The constancy of κ_8 on the plateau is preserved better in the case $\kappa_9 \ge 0.2$ than in the case $\kappa_9 = 0$ (cf. Figs. 2, 3, 4 and 5).
- The base of the NSR boundary in the case $\kappa_9 \ge 0.2$ is shifted in the positive direction of the κ_1 axis, compare Fig. 2 with the others. This base is again represented by a parallelogram. If we define the geometric center

of this parallelogram as the point of the intersection of the diagonals, we can see that this center now has the coordinates $\kappa_{1c} = 0.6, \kappa_{2c} = 0$ (in Fig. 2 we have $\kappa_{1c} = \kappa_{2c} = 0$).

Some schemes for viscous flow problems have the useful property that their stability region becomes larger for positive μ, see the examples of such schemes for the two-dimensional advection-diffusion equation (1.1) in [16]. This extension of the stability regions in the viscous case enables one to use larger values of the Courant numbers than those allowed by the stability condition for the inviscid case. The present scheme (3.3)-(3.4) does not possess this property, as following from the Figures. Therefore, an additional stabilization of the Jameson's scheme (3.1),(3.3) is desirable for increasing its computational efficiency. V.N. Vatsa [4] has implemented for this purpose the implicit residual averaging and the enthalpy damping.

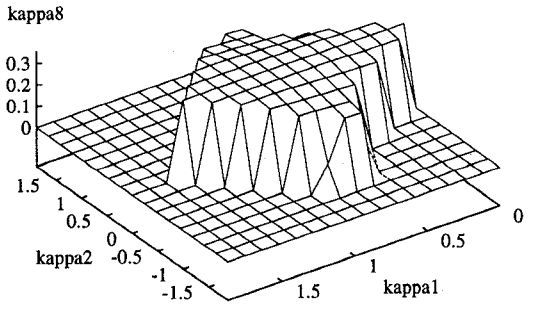

Figure 3: $\kappa_8 = \kappa_8(\kappa_1, \kappa_2)$, $\kappa_3 = \kappa_4 = 0$, $\kappa_5 = \kappa_6 = 1$, $\kappa_7 = 1.4$, $\kappa_9 = 1/0.72$.

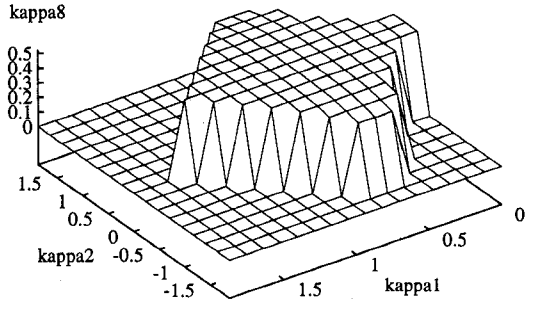

Figure 4: $\kappa_8 = \kappa_8(\kappa_1, \kappa_2)$, $\kappa_3 = \kappa_4 = 0$, $\kappa_5 = \kappa_6 = 1$, $\kappa_7 = 1.4$, $\kappa_9 = 0.5$.

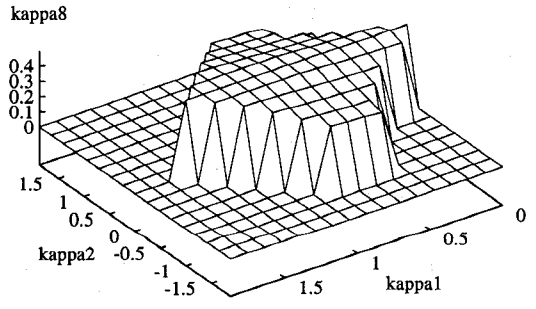

Figure 5: $\kappa_8 = \kappa_8(\kappa_1, \kappa_2)$, $\kappa_3 = \kappa_4 = 0$, $\kappa_5 = \kappa_6 = 1$, $\kappa_7 = 1.4$, $\kappa_9 = 1.0$.

6 Conclusions

We have shown above that a reasonable combination of the advanced techniques of symbolic computation and numerical analysis offers the way in which one can get an efficient tool for the solution of the difficult problem of the stability analyses of difference schemes for the three-dimensional compressible Navier-Stokes equations. Currently some of us are developing a REDUCE package, called StablePDE [17], for performing the stability analysis of lineair difference schemes for PDEs. StablePDE is compatible with Liska's FIDE package [18]. Our package can be seen as an extension of FIDE with respect to stablility analysis. The stability investigations of Jameson's schemes, which were presented above, can be seen as an application of StablePDE.

One of the directions for future research in this area is improvement of the computational speed at the numerical stages of the above outlined strategy under the simultaneous satisfaction of the requirement that roundoff errors remain at a sufficiently low level.

This work will create the necessary prerequisites for attacking the highly difficult problem of stability analysis of difference schemes on general curvilinear grids for the 3D Navier-Stokes equations.

Acknowledgements

The financial support of the Department of Computer Science of the University of Twente to one of us (E.V.V.) for visiting Enschede is gratefully acknowledged. It largely facilitated our joint research.

We express our gratitude to dr. R. Liska for his assistance in making StablePDE and FIDE compatible. The discussions with dr. R. van Damme and dr. V. Goldman during the course of our research have been helpful. Dr. van Damme's permission to use his HP 9000/735 machine for part of our computations is gratefully acknowledged as well.

References

[1] R.W. MacCormack. *On efficient numerical methods for solving the Navier-Stokes equations in three dimensions.* In: The Second Japan-Soviet Union Joint Symposium on Computational Fluid Dynamics, August 27-31, 1990, Tsukuba, Japan / Eds. Y. Yoshizawa and K. Oshima. Proceedings, Vol. II. Published by the Japan Society of Computational Fluid Dynamics, Tsukuba, 1991, p.1-13

[2] A. Jameson, W. Schmidt, and E. Turkel. *Numerical solution of the Euler equations by finite volume methods using Runge-Kutta time stepping schemes,* AIAA Paper, No. 1259, 1981.

[3] R.W. MacCormack, *The effect of viscosity in hypervelocity impact cratering,* AIAA Paper, No. 354, 1969.

[4] V.N. Vatsa. *Accurate numerical solutions for transonic viscous flow over finite wings.* J. Aircraft, 1987, vol. 24, No. 6, p. 377-385.

[5] V.G. Ganzha and E.V. Vorozhtsov. On the stability of Jameson's schemes. In: Bridging Mind and Model: Papers in Applied Mathematics / Ed. P.J. Costa. St. Thomas Technology Press, St. Paul, MN, USA, 1994, p. 237-300.

[6] V.G. Ganzha and E.V. Vorozhtsov. *Symbolic-numerical computation of the stability regions for Jameson's schemes.* In: Proceedings of the Internat. IMACS Symposium on Symbolic Computation, June 14-17, 1993, Lille, France / Eds. G. Jacob, N.E. Oussous and S. Steinberg. Published by IMACS, Lille, 1993, p. 241-246.

[7] V.G. Ganzha, E.V. Vorozhtsov and J.A. van Hulzen. *A new symbolic-numeric approach to stability analysis of difference schemes.* In: Proceedings ISSAC '92 / Ed. P.S. Wang. ACM Press, New York, 1992, p. 9-15.

[8] R.F. Warming, R.M. Beam, and B.J. Hyett. *Diagonalization and simultaneous symmetrization of the gas - dynamic matrices.* Mathematics of Computation, 1975, vol. 29. No. 132, p.1037-1045

[9] A.C. Hearn. *REDUCE 3.5, User's Manual.* Rand Corporation, Santa Monica, Cal., 1993.

[10] B.L. Gates. *GENTRAN User's Manual, REDUCE Version.* Rand Corporation, Santa Monica, Cal., 1991.

[11] J.A. van Hulzen. *SCOPE 1.5: A Source Code Optimization PackagE for REDUCE 3.5 — User's Manual.* Memorandum INF-94-17, University of Twente, Department of Computer Science (May 1994).

[12] J.A. van Hulzen, B.J.A. Hulshof, B.L. Gates and M.C. van Heerwaarden. *A code optimization package for REDUCE.* In: Proceedings ISSAC '89 / Ed. G.H.Gonnet. ACM Press, New York, 1989, p. 163-170.

[13] T. Williams and C. Kelley. *GNUPLOT: An interactive plotting program, version 3.5.* August 1993.

[14] B. Baldwin and H. Lomax. *Thin layer approximation and algebraic model for separated turbulent flows,* AIAA Paper, No. 78-257, 1978.

[15] B. York and D. Knight. *Calculation of a class of two-dimensional turbulent boundary layer flows using the Baldwin-Lomax model,* AIAA Paper, No. 85-0126, 1985, p. 1-9.

[16] E.V. Vorozhtsov and S.I. Mazurik. *A method for an automatic search for difference schemes with the biggest volume of the stability region among the schemes of a given family. 2. Application to two-dimensional problems.* Preprint of the Institute of Theoretical and Applied Mechanics of the USSR Academy of Sciences Siberian Division (in Russian), No. 34, Novosibirsk, 1987, p. 1-50.

[17] J. Boers. *StablePDE: A REDUCE package for the stability analysis of lineair difference schemes for PDEs.* Master's thesis, University of Twente, Department of Computer Science, 1994 (in preparation).

[18] R. Liska and L. Drska. *FIDE: A REDUCE package for automation of FInite difference method for solving pDE.* In: Proceedings ISSAC '90 / Eds. S. Watanabe and M. Nagata. ACM Press, New York, 1990. p. 169-176.